Molecular Crystals and Liquid Crystals
Publication details, including instructions for authors and subscription information:
http://www.tandfonline.com/loi/gmcl20

Multicolor Reflection from Chiral Photonic Crystals on the Base of Alternate Right- and Left-Handed Cholesteric Liquid Crystal Layers

A. H. Gevorgyan [a]
[a] Yerevan State University, Yerevan, Armenia
Version of record first published: 11 May 2012.

To cite this article: A. H. Gevorgyan (2012): Multicolor Reflection from Chiral Photonic Crystals on the Base of Alternate Right- and Left-Handed Cholesteric Liquid Crystal Layers, Molecular Crystals and Liquid Crystals, 559:1, 76-90

To link to this article: http://dx.doi.org/10.1080/15421406.2012.658686

Mol. Cryst. Liq. Cryst., Vol. 559: pp. 76–90, 2012

ISSN: 1542-1406 print/1563-5287 online
DOI: 10.1080/15421406.2012.658686

Taylor & Francis
Taylor & Francis Group

Multicolor Reflection from Chiral Photonic Crystals on the Base of Alternate Right- and Left-Handed Cholesteric Liquid Crystal Layers

A. H. GEVORGYAN*

Yerevan State University, Yerevan, Armenia

In this paper, we investigated the optical properties of stacked right- and left-hand chiral photonic crystal layers. The reflection spectra peculiarities of this system were investigated showing that, in contrast to a single CLC layer, there are multiple PBGs. The Eigen polarizations (EP) of the system are degenerated and the polarization plane rotation decreases if the system thickness is increased; the rotation sign depends on the first sublayer chirality sign. We also investigated the influence of sublayer thicknesses, sublayer local dielectric anisotropies, and sublayer helix pitches on the reflection peculiarities of the system.

Keywords Cholesteric liquid crystals; color display; diffraction; eigen polarizations; photonic band gap; photonics; red-green-blue-reflection; reflection; transmission

PACS numbers 42.70.Df; 42.70.Qs; 61.30.-v; 78.67.-n

Introduction

The current research and development in optical materials for photonic applications are largely centered on structured materials that exhibit unique physical and optical properties [1–3]. In particular, photonic crystals (PCs) draw an abundance of attention due to their interesting physical properties and their relevance in the development of new electro-optical and photonic devices. PCs exhibit photonic band gaps (PBGs), which prevent light propagation in certain frequency ranges. PBGs can be suitably tuned by modifying the internal stacked structure [4–7]. These structures, designed artificially or in a self assembling manner, can be prepared with properties leading to many challenging problems of a theoretical or applied nature. Optical devices constructed from PCs result in intelligent, multifunctional and tunable optics, possessing positive traits such as compactness, small losses, high reliability and high compatibility with other devices. PCs with tunable parameters are of particular interest. A classic example of PCs with easily tunable parameters is cholesteric liquid crystals (CLCs). A CLC is a self-assembled photonic crystal formed by rod-like molecules, including chiral molecules, which arrange themselves in a helical fashion. The CLC has a single photonic band gap (PBG) and an associated one-color reflection band for circularly polarized light with the same handedness as the CLC helix (at normal light incidence). The parameters of the CLCs can be easily tuned by external electrical or magnetic

*Address correspondence to A. H. Gevorgyan, Chair of General Physics, Department of Physics, Yerevan State University, 1 A. Manoogian Str., Yerevan 0025, Armenia. Tel: + 374 10 628008. E-mail: agevorgyan@ysu.am

fields, by thermal gradient, IR radiation, etc. A suitable manipulation of the CLCs layer parameters will allow for fine-tuning of the PBG and other characteristics. Recently, PCs with multiple PBGs are of great interest as they are widely applicable, particularly, within the display industry.

The formation of multiple PBGs in one-dimensional stacked structures containing CLC layers and isotropic/anisotropic layers, as well as quasi-periodic systems characterized by Fibonacci numbers have been reported theoretically and experimentally [8–14], and their investigations are still concrete. In paper [15], the reflection peculiarities of the stack of two-layer CLC, which differ from each other by the helix sign, are theoretically investigated and it is shown that this system allows for the possibility to obtain a 100% polarized diffraction reflection. This system's EPs have degenerated. On the other hand, it was experimentally demonstrated that the introduction of photopolymerizable monomers into a cholesteric medium can, after UV light curing, generate regions with helicity inversion [16,17]. Such polymer-cholesteric gels behave as an infrared hyper-reflective network almost independent of the light polarization. Paper [18] shows the experimental investigation of novel hybrid structures composed of a dye-doped low-molecular-weight CLC sandwiched by multilayered polymer CLC films with right- and left-handed polymer CLC layers and evaluated their lasing characteristics. It was shown that lasing can be observed with an extremely reduced threshold.

The dielectric anisotropy, $\Delta = \frac{\varepsilon_1 - \varepsilon_2}{2}$, for the ordinary CLCs is of order 0.5 and smaller. But recently made artificial crystals (metamaterials) have a dielectric anisotropy that can be varied in a large interval. It seems that helical periodic media, like CLCs, with large local anisotropy can be created on their base. Such media with comparatively weak anisotropy have previously been created [19,20]. Recently, interest in CLCs enriched with nanoparticles has been increased (see, [21], and references cited therein). The presence of nanoparticles (either ferroelectric or ferromagnetic) in the CLC structure leads to: an essential increase of its local (both dielectric and magnetic) anisotropy, a significant change of the *isotropic phase-liquid phase* transition temperature, a significant change of the photonic band gap frequency width and the frequency localization, a change of the CLC elasticity coefficients, a significant increase of the CLC tuning possibilities, etc.

It follows that investigation of the optical peculiarities of a stack of right- and left-handed chiral photonic crystal layers for various values of its local dielectric anisotropy can have great interest.

This paper discusses the investigation of the reflection and polarization properties of the multilayered structures representing a stack of right- and left- hand chiral photonic crystal layers (Fig. 1). Many new, interesting peculiarities of this system were found, which also can have important applications.

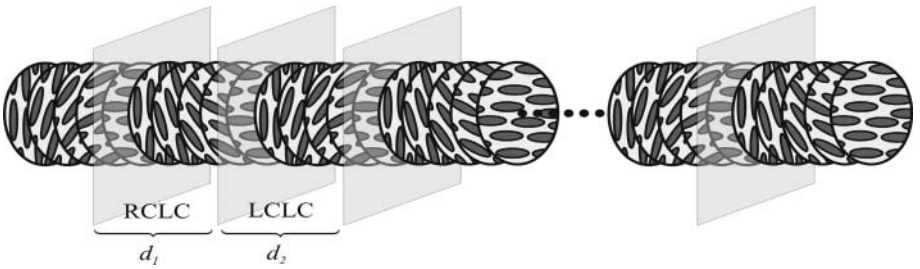

Figure 1. A sketch diagram of a model of stacked right- and left-hand cholesteric liquid crystal layers.

The rest of this paper is organized as follows: in the second (following) section, the methodology and the basic principles for the calculation of reflection and transmission matrices as well as of EPs are formulated. In the third section, we carry out the numerical calculations and analyze the reflection (transmission) and polarization plane rotation, polarization ellipticity, and EPs azimuth and ellipticity spectra peculiarities of the proposed system. Concluding remarks are given in the fourth section.

The Method of the Analysis

This problem is solved by Ambartsumian's layer addition modified method adjusted to solution of such problems (see, [14, 15]).

According to *Ambartsumian's layer addition modified method*, if there is a system consisting of two adjacent (from left to right) layers, A and B, then the reflection transmission matrices of the system, $A + B$, viz. $\widehat{R}_{A+B}$ and $\widehat{T}_{A+B}$, are determined in terms of similar matrices of its component layers by the matrix equations:

$$\begin{aligned}\hat{R}_{A+B} &= \hat{R}_A + \tilde{\hat{T}}_A \hat{R}_B [\hat{I} - \tilde{\hat{R}}_A \hat{R}_B]^{-1} \hat{T}_A,\\ \hat{T}_{A+B} &= \hat{T}_B [\hat{I} - \tilde{\hat{R}}_A \hat{R}_B]^{-1} \hat{T}_A,\end{aligned} \tag{1}$$

where $\hat{I}$ is the unit matrix, and the tilde denotes the corresponding reflection and transmission matrices for the reverse direction of light propagation. For instance, in the case where the layer of the medium is bordered from its both sides by the same medium, the reflection and transmission matrices for the light incident from the left and from the right are connected to one another through the relations:

$$\begin{aligned}\tilde{\hat{T}} &= \hat{F}^{-1} \hat{T} \hat{F},\\ \tilde{\hat{R}} &= \hat{F}^{-1} \hat{R} \hat{F},\end{aligned} \tag{2}$$

where $\hat{F} = \begin{pmatrix} 1 & 0 \\ 0 & -1 \end{pmatrix}$ for linear base polarizations and $\hat{F} = \begin{pmatrix} 0 & 1 \\ 1 & 0 \end{pmatrix}$ for circular base polarizations.

The exact reflection and transmission matrices for a finite ***CLC layer*** (at light normal incidence) are well known [22]. We present the solution of the boundary problem of light transmission through the single finite layer of CLC in the form:

$$\vec{E}_r = \hat{R} \vec{E}_i, \quad \vec{E}_t = \hat{T} \vec{E}_i, \tag{3}$$

where the indices i, r and t denote the incident, reflected and transmitted waves fields, $\hat{R}$ and $\hat{T}$ are the reflection and transmission matrices, $\vec{E}_{i,r,t} = E^+_{i,r,t} \vec{n}_+ + E^-_{i,r,t} \vec{n}_- = \begin{bmatrix} E^+_{i,r,t} \\ E^-_{i,r,t} \end{bmatrix}$, $\vec{n}_\pm = (\vec{x} \pm i\vec{y})/\sqrt{2}$, and for the matrices $\hat{R}$ и $\hat{T}$ (according to [22,23]) we have:

$$\begin{aligned} R_{jj} = {} & \{\chi^2 r_1 r_2 (c_1 c_2 - 1) + 2u^2 [r_1 r_2 (2\chi^2 (m_1 - \delta_\varepsilon \delta_\mu) - \gamma^2) - g_1 g_2 \gamma^2] s_1 s_2 \\ & - iu\sqrt{\alpha}\gamma (p_1 s_1 c_2 + p_2 s_2 c_1)\}/\Delta, \; R_{jk} = \{\eta_j q_2 \chi r_2 \sqrt{\alpha} (c_1 c_2 - 1) + 4u^2 \sqrt{\alpha} \\ & \times [q_1 \gamma^2 \sqrt{\alpha} - \eta_j \chi [g_1 (2\chi^2 - m_2) + m_1 (\alpha \delta_\mu + \delta_\varepsilon) + q_2 (\delta_\mu^2 - \alpha \delta_\varepsilon^2)]] s_1 s_2 \\ & + iu\gamma\sqrt{\alpha} - (v_1 s_1 c_2 - v_2 s_2 c_1)\}/\Delta, \; T_{jj} = \gamma\sqrt{\alpha} \exp(-\eta_j a d)\{(\gamma\sqrt{\alpha} + \eta_j \chi r_1) c_1 \end{aligned}$$

$$+(\gamma\sqrt{\alpha}-\eta_j\chi r_1)c_2 - iu[(t_1+2\eta_j l_1\sqrt{\alpha})s_1+(t_2+2\eta_j l_2\sqrt{\alpha})s_2]\}/\Delta,\ T_{jk}=\gamma$$
$$\times\sqrt{\alpha}\exp(-\eta_j ad)\{\sqrt{\alpha}q_2(c_1-c_2) - iu[(r_1q_2+\gamma g_2)s_1-(r_1q_2-\gamma g_2)s_2]\}/\Delta,$$
$$j,k=1,2;\ j\neq k, \tag{4}$$

where $\Delta=-\chi^2r_2^2+(\chi^2r_2^2+2\alpha\gamma^2)c_1c_2+2u^2\{\gamma^2g_2^2-r_1^2q_2^2-2\chi^2[m_1(r_1^2+4\alpha)+r_2^2\delta_\varepsilon\delta_\mu-2\alpha q_2^2]\}s_1s_2-2iu\gamma\sqrt{\alpha}(t_1s_1c_2+t_2s_2c_1)$, $p_{1,2}=r_1w_{1,2}\pm q_2g_1$, $g_{1,2}=\delta_\mu\pm\alpha\delta_\varepsilon$, $q_{1,2}=\delta_\mu\pm\delta_\varepsilon$, $v_{1,2}=r_2q_2\pm\gamma g_1+2\sqrt{\alpha}\eta_jq_1\chi$, $t_{1,2}=r_1w_{1,2}\pm q_2g_2$, $m_{1,2}=1\pm\chi^2$, $w_{1,2}=\gamma\pm2\chi^2$, $l_{1,2}=\gamma\pm2$, $s_{1,2}=\sin(k_{1,2}d)/(k_{1,2}d)$, $c_{1,2}=\cos(k_{1,2}d)$, $k_{1,2}=2\pi\sqrt{\varepsilon_m\mu_m}b^{\pm}/\lambda$, $b^{\pm}=\sqrt{1+\chi^2-\delta_\varepsilon\delta_\mu\pm\gamma}$, $\gamma=\sqrt{4\chi^2+(\delta_\varepsilon-\delta_\mu)^2}$, $\eta_j=(-1)^j$, $r_{1,2}=1\pm\alpha$, $\alpha=\sqrt{\frac{\varepsilon_m}{\mu_m\varepsilon}}$, ε is the dielectric permittivity of the surroundings of the CLC layer, $u=\pi d\sqrt{\varepsilon_m\mu_m}/\lambda$, d is CLC layer thickness, $a=2\pi/p$, p is the helix pitch, $\chi=\lambda/(p\sqrt{\varepsilon_m\mu_m})$, λ is the wavelength in vacuum, $\varepsilon_m=(\varepsilon_1+\varepsilon_2)/2$, $\delta_\varepsilon=(\varepsilon_1-\varepsilon_2)/(\varepsilon_1+\varepsilon_2)$ where ε_1 and ε_2 are the principal values of the local dielectric permittivity tensor, and $\mu_m=(\mu_1+\mu_2)/2$, $\delta_\mu=(\mu_1-\mu_2)/(\mu_1+\mu_2)$ where μ_1 and μ_2 are the principal values of the local magnetic permittivity tensor.

Matrices $\hat{R}$ and $\hat{T}$ for CLC layer are simplified for $\alpha=1$. For this case, we have:

$$R_{jj}=iu\delta^2(s_1a_2-s_2a_1)/\Delta,\ R_{jk}=iu\delta(h_ks_1a_2+h_js_2a_1)/\Delta,$$
$$T_{jj}=\exp(-\eta_j ad)(h_ja_2+h_ka_1)/\Delta,\ T_{jk}=-\delta\exp(-\eta_j ad)(a_1-a_2)/\Delta, \tag{5}$$

where $\Delta=2\gamma a_1a_2$, $a_{1,2}=c_{1,2}\mp iul_{1,2}s_{1,2}$, $h_{1,2}=\gamma\pm2\chi$.

The calculations of transmission (reflection) through the stacked right- and left-hand CLC layers were carried out on the base of matrix equations (1), applying them in turn as we were adding a new CLC layer, considered layer "B", to the stack, considered the "A" layer. Therefore, to organize the calculations well system (1) was presented in the form of the system of the following difference matrix equations:

$$\hat{R}_j=\hat{r}_j+\tilde{\hat{t}}_j\hat{R}_{j-1}(\hat{I}-\tilde{\hat{r}}_j\hat{R}_{j-1})^{-1}\hat{t}_j,$$
$$\hat{T}_j=\hat{T}_{j-1}(\hat{I}-\tilde{\hat{r}}_j\hat{R}_{j-1})^{-1}\hat{t}_j, \tag{6}$$

with $\hat{R}_0=\hat{0}$ and $\hat{T}_0=\hat{I}$. Here $\hat{R}_j$, $\hat{T}_j$, $\hat{R}_{j-1}$ and $\hat{T}_{j-1}$ are the reflection and transmission matrices for the system consisting of *j-th* and $(j-1)$-th sublayers, respectively; and $\hat{r}_j$, $\hat{t}_j$ are the reflection and transmission matrices, respectively, for an *j*-th sublayer; $\hat{0}$ is the zero matrix.

Let us now consider the EPs. The EPs are the two polarizations of the incident light, which do not change when light transmits through the system [14,24]. The EPs and Eigen values (the amplitude transmission and reflection coefficients for the incident light with EPs) deliver considerable information about the peculiarities of light interaction with the system. Therefore, the calculation of EPs and Eigen values of every optical device is important. It follows from the definition that EPs must be connected with the polarizations of the excited internal waves (the Eigen modes) aroused in the medium. In the majority of cases, they coincide with the polarizations of the Eigen modes. Naturally, there are certain differences in the general case: only two EPs exist, the number of eigen modes can be more than two, and the polarizations of these modes can differ from each other (for the non-reciprocity media, for instance).

The EPs automatically take the influence of the dielectric borders into account. As it is known (in particular, at the normal incidence), the EPs of either CLC or gyrotropic media

coincide with the orthogonal circular polarizations; meanwhile, they coincide with the orthogonal linear polarizations for the non-gyrotropic media. It follows from the above that investigation of the EPs peculiarities is especially important in the case of inhomogeneous media for which the exact solution of the problem is unknown.

Denoting the ratio of the complex field components by $\chi_i = E_i^-/E_i^+$ for the incidence wave at the entrance of the system, and the same ratio at the exit by $\chi_t = E_t^-/E_t^+$, and taking into account that: $\begin{bmatrix} E_t^+ \\ E_t^- \end{bmatrix} = \begin{bmatrix} T_{11} & T_{12} \\ T_{21} & T_{22} \end{bmatrix} \begin{bmatrix} E_i^+ \\ E_i^- \end{bmatrix}$, we find that:

$$\chi_t = (T_{22}\chi_i + T_{21})/(T_{12}\chi_i + T_{11}), \tag{7}$$

where T_{ij} are the elements of the total system transmission matrix.

The function, $\chi_t = f(\chi_i)$, is called *polarization transfer function* [24] and it holds information about polarization ellipse transformation when light is transmitted through the system. Every optical system has two EPs, which are obtained through substitution χ_t from equation (2) into the equation $\chi_i = \chi_t$, resulting in:

$$\chi_{1,2} = \frac{T_{22} - T_{11} \pm \sqrt{(T_{22} - T_{11})^2 + 4T_{12}T_{21}}}{2T_{12}}. \tag{8}$$

The ellipticities, $e_{1,2}$, and the azimuths, $\psi_{1,2}$, of the EPs are expressed by $\chi_{1,2}$ through the following formulae:

$$\psi_{1,2} = -\frac{1}{2}\arg(\chi_{1,2}),\ e_{1,2} = arctg\left(\frac{|\chi_{1,2}| - 1}{|\chi_{1,2}| + 1}\right). \tag{9}$$

Results and Discussion

We analyzed the spectral properties of the multi-layered structures of right- and left-hand chiral photonic crystal layers as presented in Fig. 1. The main values of dielectric and magnetic permittivity tensors of CLC, in general, were taken to be $\varepsilon_1 = 2.29$, $\varepsilon_2 = 2.143$, $\mu_1 = 1.2$, and $\mu_2 = 1.1$. The *CLC layers* helixes are right- and left-handed and with pitches of $p_{1,2} = \pm 420$ nm. Thus, the incident onto a single *CLC layer* with, for instance, right helix light with the right circular polarization (RCP) has a PBG while light with the left circular polarization (LCP) does not.

Reflection Spectra and Spectra of Polarization Characteristics

Here we investigated the case where the sublayers of the two types have the same parameters and only differ from each other by the helicity sign. Figure 2 presents the reflection spectra in the case of normal light incidence for various sublayer numbers, *s,* of the system. The incident light has RCP (dashed lines) and LCP (solid lines). Consider the case $\alpha = 1$.

As seen in this Figure, in contrast to a single CLC layer, this system has multiple PBGs. At zero order reflection, the system manifests itself with three diffraction reflection peaks (red-green-blue- reflection). If the sublayer number of the system is even, this system does not manifest selectivity in respect with the incident wave polarization. On the other hand, if the sublayer number is odd, the system manifests strong selectivity with respect to the incident wave polarization, particularly with the circular polarization (the reflection spectra of the orthogonal linear polarizations practically coincide). The difference of the orthogonal

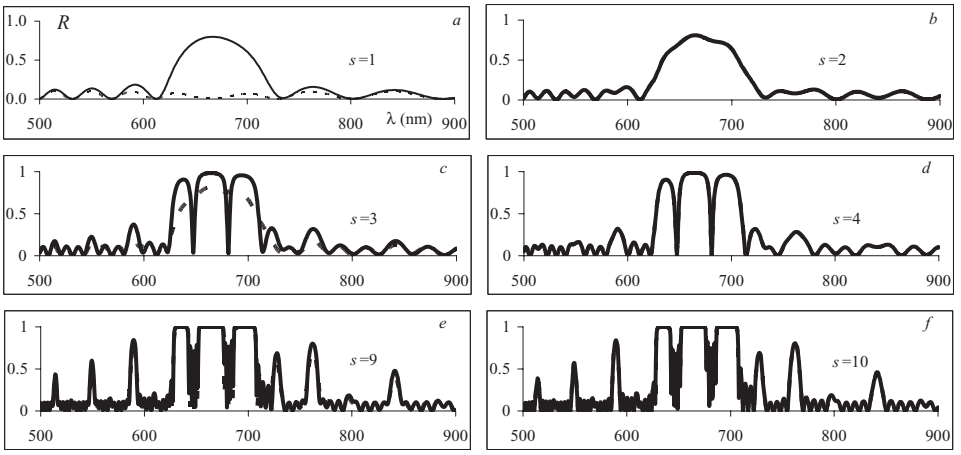

Figure 2. The reflection spectra for various numbers of sublayers, s. The incident light has RCP (dashed lines) and LCP (solid lines). $d_1 = d_2 = 2500$ nm,$\alpha = 1$.

circular polarizations in the incident wave reflection in the region of the diffraction reflection vanishes when the sublayer number in the system increases. Also, the diffraction efficiency of the other reflection orders increases if the sublayer number increases.

Next, we consider the polarization characteristics. Figure 3 presents the polarization plane rotation spectra (ψ, solid lines) and the spectra of the polarization ellipticity (e, dashed lines) for various sublayer numbers, s, in the system for the normal wave incidence. The incident light is linearly polarized. Comparison of rotation curves for various sublayer numbers shows the rotation in the system is higher by one order for an odd number of sublayers than that of the even number of sublayers, which is expected. Let us note that for an even sublayer number the polarization plane rotation is not zero and significantly differs

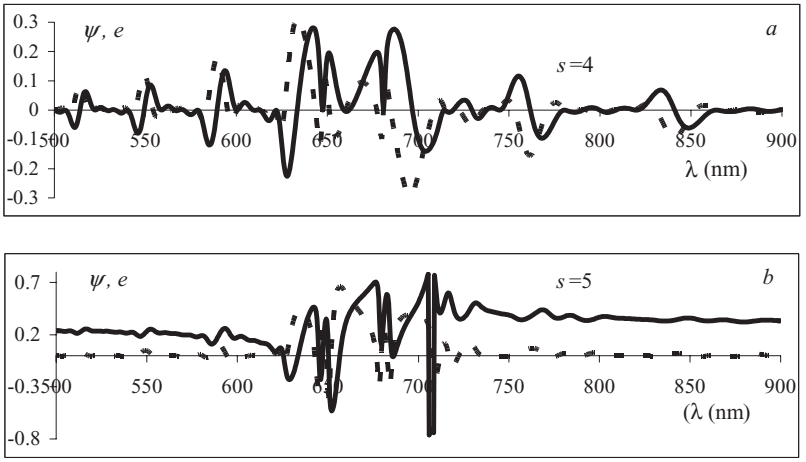

Figure 3. Polarization plane rotation spectra (ψ, solid lines) and polarization ellipticity spectra (e, dashed lines) for various numbers of sublayers, s. The incident light is linearly polarized. $d_1 = d_2 = 2500$ nm,$\alpha = 1$.

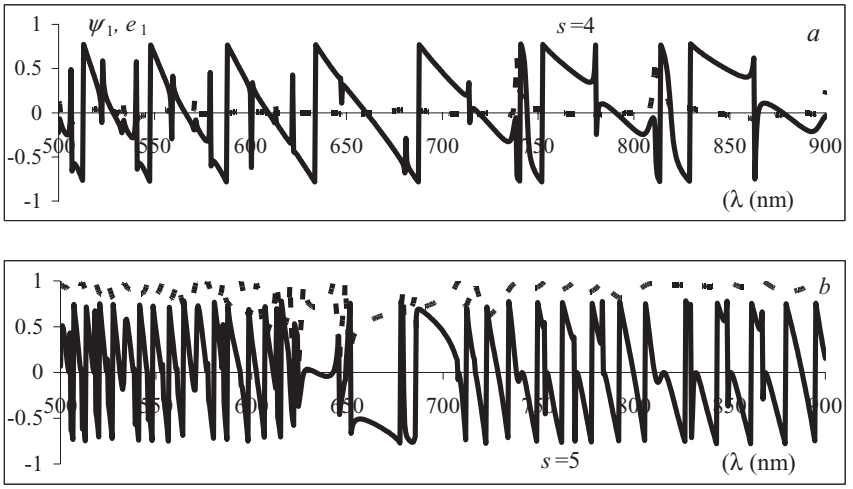

Figure 4. The azimuths (ψ_1, solid lines) and ellipticity (e_1, dashed lines) spectra of the EPs for various numbers of sublayers, *s*. $d_1 = d_2 = 2500$ nm,$\alpha = 1$.

from zero in the PBG. This is stipulated not only by diffraction multireflections from each border of each sublayer, but also by dependences of reflection and transmission in each sublayer on the azimuth and polarization ellipticity of the light incident on that layer.

Figure 4 presents the spectra of the azimuths (ψ_1, solid lines) and ellipticities (e_1, dashed lines) of the EPs for various sublayer numbers, *s,* in the system for the normal incidence of light. If the sublayer number is even, the EPs are degenerated (both EPs coincide); if the sublayer number is odd, the EPs are quasicircular polarizations, which are quasiorthogonal outside the PBG.

It should be noted that the main peculiarity of the subject system is its optical characteristic's strong dependence (especially the polarization ones) on the sublayer number in the system and helical nature of the first sublayer (i.e. whether its helix is right handed or left handed). First it must be noted that in contrast to the amplitude characteristics, which practically lose their sensitivity due to the change in sublayer number and helical nature character of the first sublayer in the system for $s > 10$, the polarization characteristics do not lose this sensitivity. If the sublayer number increases, these characteristics are changed with jumps that slowly changing amplitudes. Such a system is particularly unique, for the sign of its polarization plane rotation depends on the helicity sign of the first sublayer (for the even sublayer number, too) and in contrast to the ordinary gyrotropic media, the polarization plane rotation magnitude can decrease (with oscillations) as the system thickness increases.

Impact of the Sublayer's Thickness

Next we consider the influence of the change of the sublayer's thickness on the reflection spectra. First, let us consider (as above) the case when the sublayers of the two types have the same parameters except for helicity signs. Figure 5 presents the density plot of the reflection spectra as a function of the sublayer thicknesses, $d = d_1 = d_2$. As the sublayer's thickness increases, the diffraction efficiency in the PBGs also increases and the PBGs shift to the long wave region. New PBGs appear and additional modulation is observed.

Figure 6 presents the density plot of the reflection spectra at another (larger) value of the medium anisotropy. As is seen in Fig. 6, for larger values of the sublayer thickness

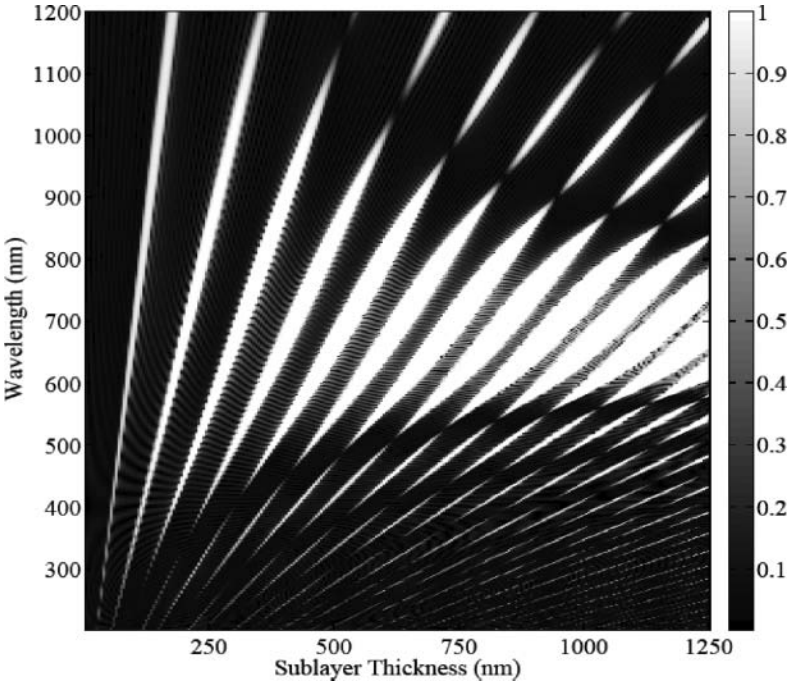

Figure 5. The density plot of the reflection spectra as a function of the sublayer thicknesses, $d = d_1 = d_2$. The incident light is of the RCP. $\varepsilon_1 = 2.5$, $\varepsilon_2 = 2.2$, $\mu_1 = 1.3$, $\mu_2 = 1$, $\alpha = 1$, $s = 25$.

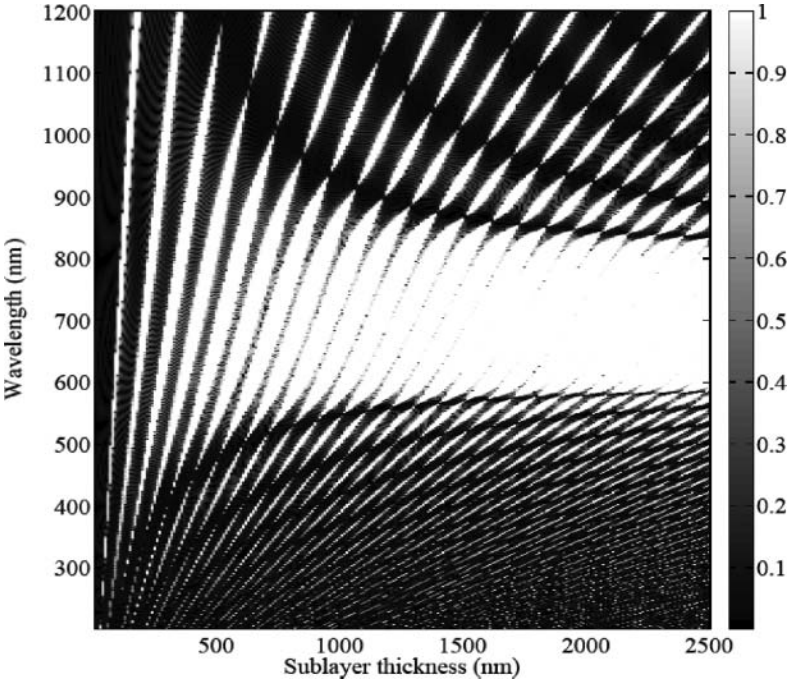

Figure 6. The density plot of the reflection spectra as a function of the sublayer thicknesses, $d = d_1 = d_2$. The incident light is of the RCP. $\varepsilon_1 = 2.5$, $\varepsilon_2 = 2.0$, $\mu_1 = 1.5$, $\mu_2 = 1.0$,$\alpha = 1$, $s = 25$.

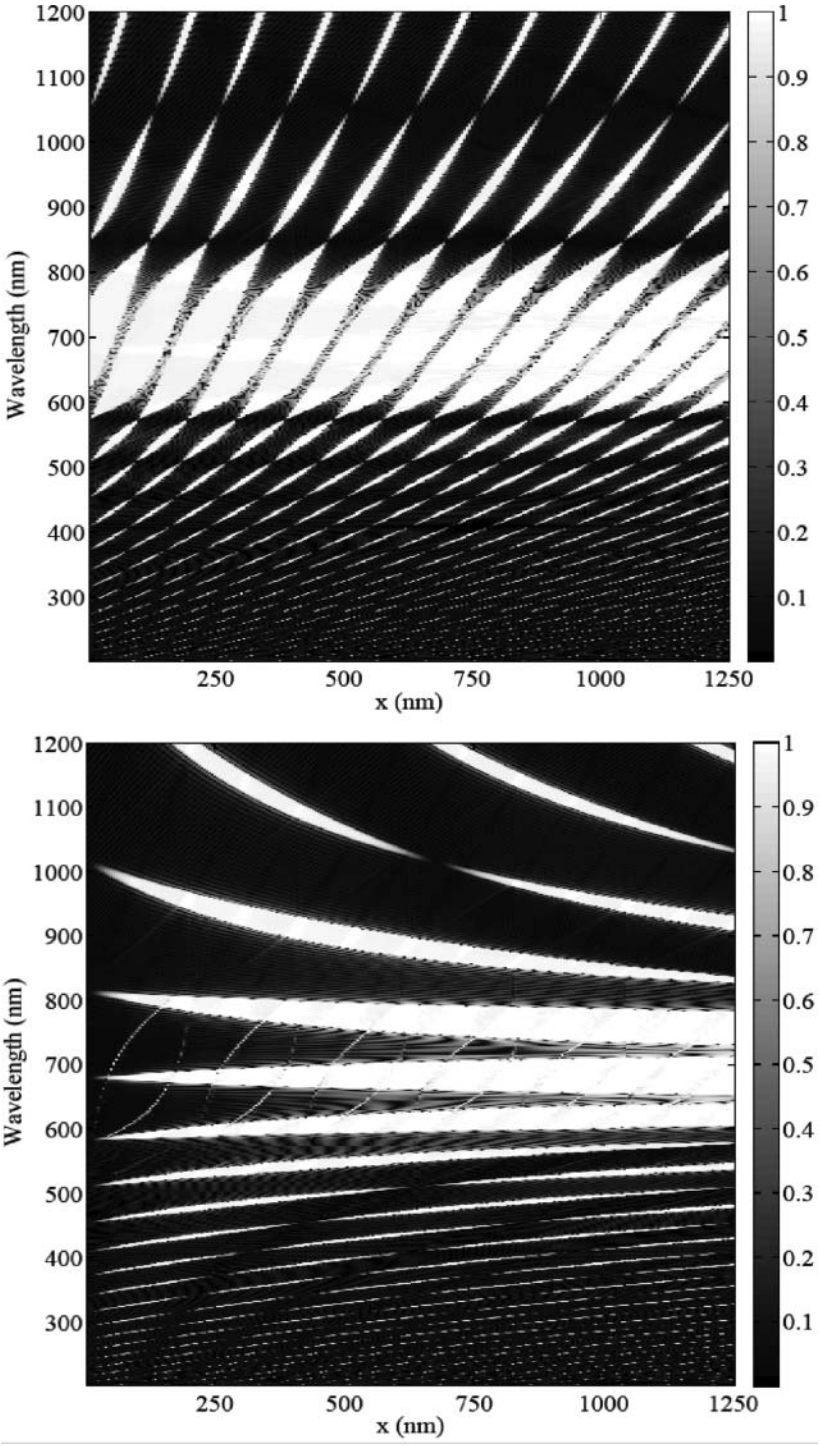

Figure 7. The density plot of the reflection spectra as a function of the sublayer thicknesses, $d_2 = x$. The incident light has the right (a) and left (b) circular polarization. $\varepsilon_1 = 2.5$, $\varepsilon_2 = 2.2$, $\mu_1 = 1.3$, $\mu_2 = 1.0$, $s = 50$, $d_1 = 1250$ nm, $\alpha = 1$.

d, a PBG of the first order is formed with borders defined by the following expression, $\lambda_{1,2} = p\sqrt{\varepsilon_{1,2}\mu_{1,2}}$, i.e. these borders coincide with the borders of the PBG for a single CLC layer.

Now we consider the case when d_1 is fixed and only $d_2 = x$ changes. In Fig. 7, the density plot of the reflection spectra as a function of the sublayer's thickness, $d_2 = x$ are presented. The incident light has right handed (a) and left handed (b) circular polarizations. If $d_1 \neq d_2$, the properties of the system essentially differ from those where $d_1 = d_2$. First, the EPs (independent of sublayer number and helicity) become quasicircular basis polarizations. The system manifests stronger selectivity of the incident wave polarizations. In this case, the reflection spectra characteristic changes (depending on changes of x) for the right handed circularly polarized incident light essentially differ from those for the left handed circularly polarized incident light. If the reflection spectra change, regularities for the right handed circularly polarized incident light practically do not change when x increases; for the left handed circularly polarized incident light, significant frequency widening of the principal (i.e. red-, green-, blue-) PBGs takes place, moreover, the frequency locations of the PBGs (except the central one) change.

Effects of Local Dielectric Anisotropy

As previously mentioned in the Introduction, the dielectric anisotropy, $\Delta = \frac{\varepsilon_1 - \varepsilon_2}{2}$, for ordinary CLCs is of order 0.5 and smaller. But recently, artificial crystals (metamaterials)

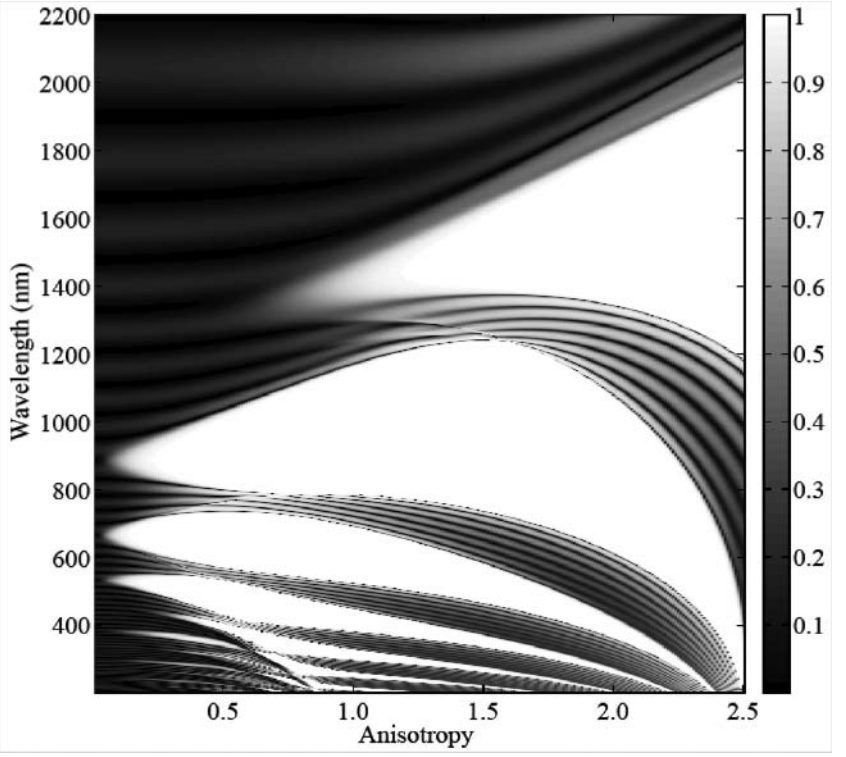

Figure 8. The density plot of the reflection spectra as a function of the anisotropy Δ. The incident light is of the RCP. s = 10, $d_1 = d_2 = 420$ nm, $\varepsilon_{01} = \varepsilon_{02} = 2.5$, $\mu_{01} = \mu_{02} = 1.0$, $\alpha = 1$.

have been made with a dielectric anisotropy that can be varied in a large interval, and helical periodic media like CLCs having huge local anisotropy, which can be created on their base.

It follows from the above that investigation of the optical peculiarities of a stack of right- and left- handed chiral photonic crystal layers for various values of its local dielectric anisotropy can have great interest. Representing the principal values of the dielectric permittivity tensor of the right and left handed CLC sublayers in the form $\varepsilon_1 = \varepsilon_{01} + \Delta$, $\varepsilon_2 = \varepsilon_{02} - \Delta$, and $\mu_1 = \mu_{01} + \Delta$, $\mu_2 = \mu_{02} - \Delta$, we investigate the influence of the anisotropy, Δ, on the reflection spectra.

Figure 8 presents the density plot of the reflection spectra as a function of the anisotropy, Δ. The incident light is circularly polarized. If the local anisotropy increases, the number of PBGs, as well as their frequency positions and frequency widths increase, as well. For larger anisotropies, the frequency widths of some PBGs begin to decrease and will even vanish. Selectivity of the incident wave polarizations appears (including the selectivity of the circular polarizations) and the reflection outside the PBG increases.

To demonstrate the possibilities of the subject system, the density plots of the reflection spectra as a function of the anisotropy, Δ, are presented below for various values of the following parameters: ε_{01}, ε_{02}, μ_{01}, and μ_{02} (see Figs. 8–11).

The following condition, $\varepsilon_1\mu_1 = \varepsilon_2\mu_2$, takes place in Fig. 9 for $\Delta = 1.25$ (this value is denoted by an arrow in the figure). For this condition, (see, for instance, [23]), a separate CLC layer does not have any PBG for the normal incidence. It follows, from this figure,

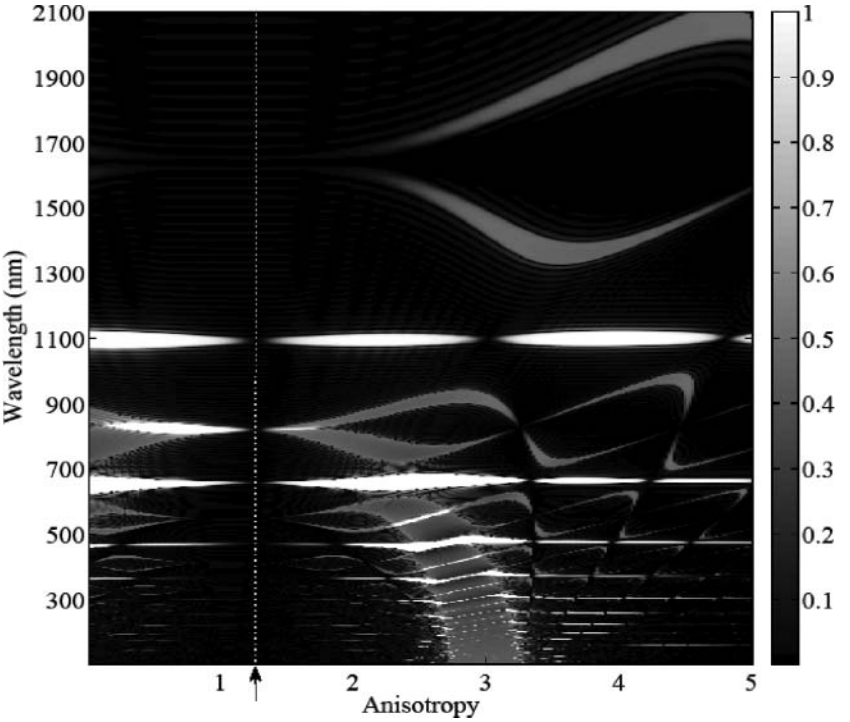

Figure 9. The density plot of the reflection spectra as a function of the anisotropy Δ. The incident light is of the RCP. $s = 5$, $d_1 = d_2 = 420\,\text{nm}$, $\varepsilon_1 = 1.25 + \Delta$, $\varepsilon_1 = 3.25 - \Delta$, $\mu_1 = 2.75 - \Delta$, $\mu_2 = 0.625 + \Delta$, $\alpha = 1$.

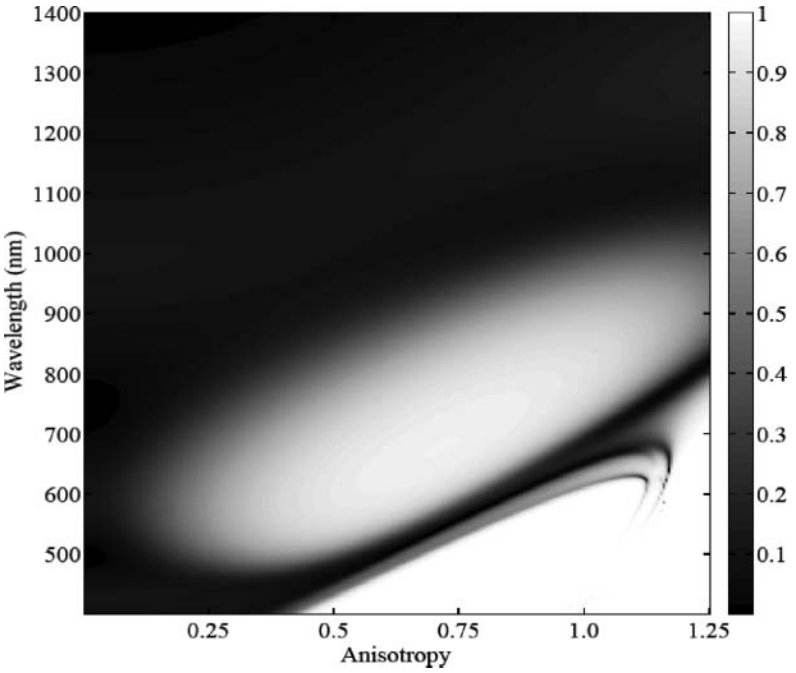

Figure 10. The density plot of the reflection spectra as a function of the anisotropy Δ. The incident light is of the RCP. $s = 5$, $d_1 = d_2 = 420\,\text{nm}$, $\varepsilon_{01} = \varepsilon_{02} = 0.5$, $\mu_{01} = \mu_{02} = 0.25$, $\alpha = 1$.

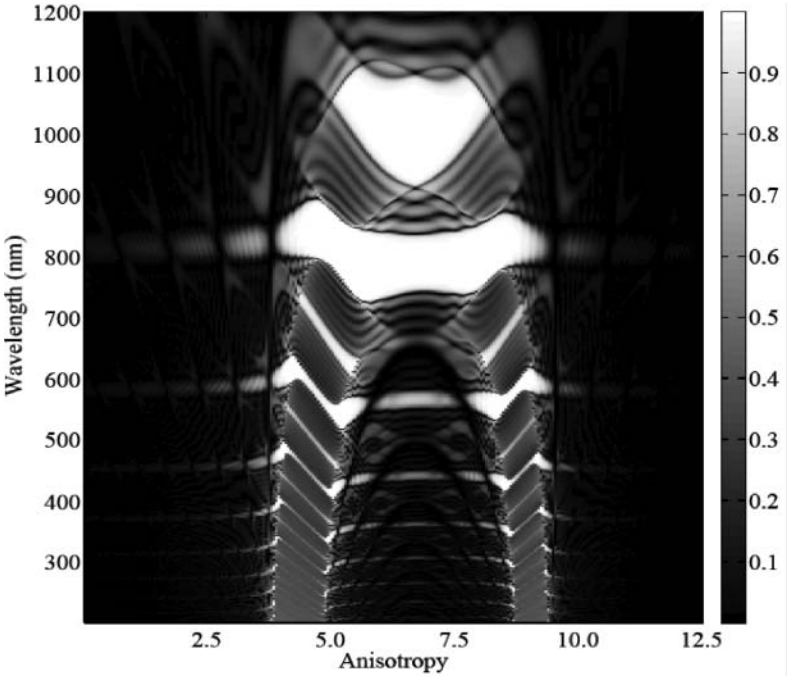

Figure 11. The density plot of the reflection spectra as a function of the anisotropy Δ. The incident light is of the RCP. $s = 10$, $d_1 = d_2 = 420\,nm$, $\varepsilon_1 = -3.75 + \Delta$, $\varepsilon_1 = 8.75 - \Delta$, $\mu_1 = 9.375 - \Delta$, $\mu_2 = -4.75 + \Delta$, $\alpha = 1$.

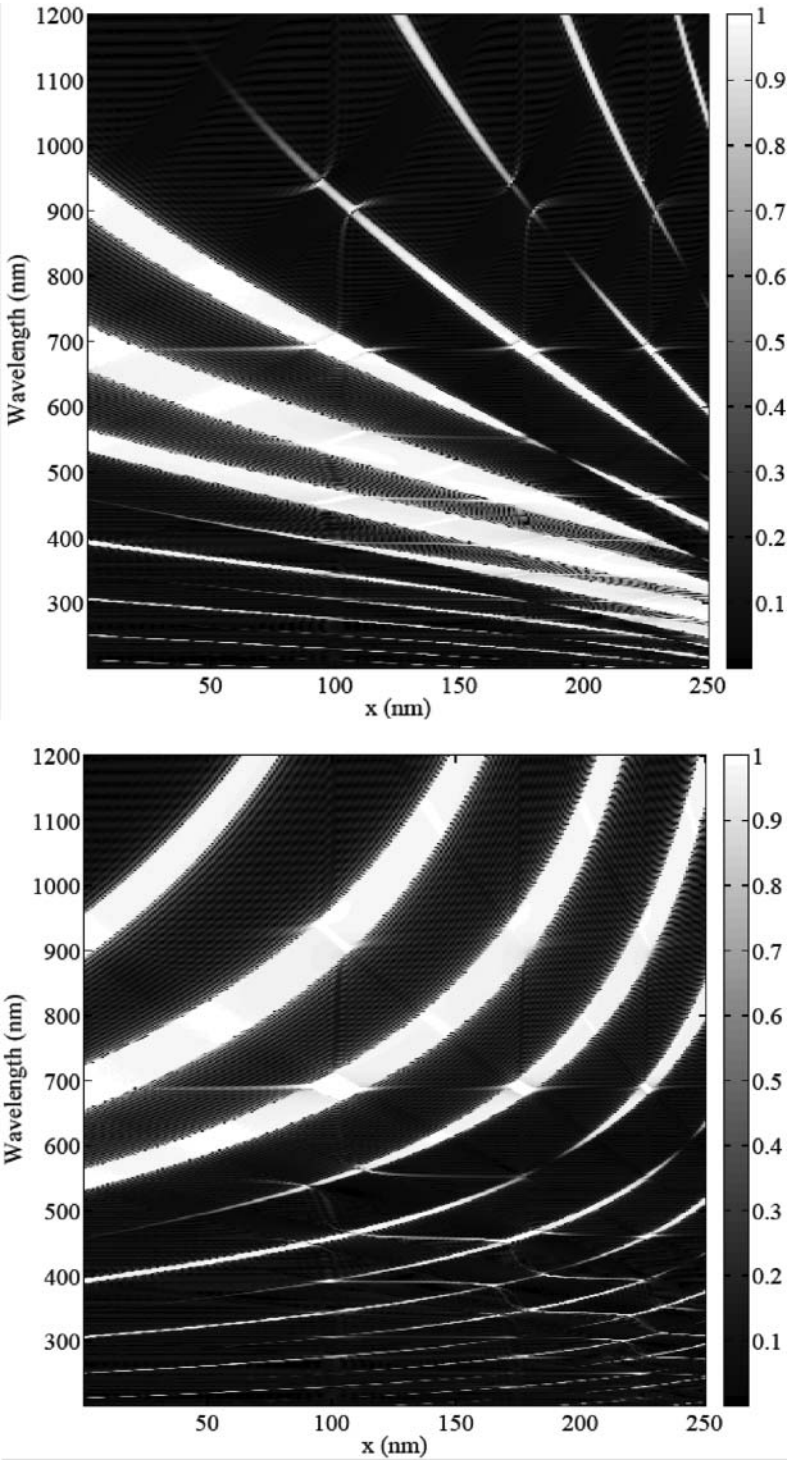

Figure 12. The density plot of the reflection spectra as a function of the pitches change x. The incident light has the LCP (a) and the RCP (b). $s = 50$, $d_1 = d_2 = 420\,\text{nm}$, $\alpha = 1$.

that stacked right- and left-hand cholesteric liquid crystal layers also have no PBG if $\varepsilon_1\mu_1 = \varepsilon_2\mu_2$.

Influence of CLC Sublayers Pitches

Next we investigated the influence of sublayer pitch changes onto the system's reflection spectra. The CLC sublayer helix pitches are presented in the forms: $p_i = (-1)^{i+1}p_0 + x$ ($p_0 > 0$, $i = 1,2$), i.e. we assume that the helix pitches of the right hand CLC sublayers increase and those of the left hand CLC sublayers decrease (by their magnitude). We also consider the influence of changes of x on the reflection spectra; Fig. 12 presents the density plot of the reflection spectra as a function of the x. The incident light has left hand circular polarization (Fig. 12(a)), and right hand polarization (Fig. 12(b)). For $|p_1| \neq |p_2|$, the reflection spectra becomes sensitive to polarization and it is as if two diffraction patterns are formed: the first is the result of the diffraction of the incidence light with the left hand circular polarization at the equidistant layers with left hand CLC sublayers, and the second is the result of the diffraction of the incidence light with the right hand circular polarization at the equidistant layers with the right hand CLC sublayers. Therefore, the principal diffraction reflection maxima for the incident light with left hand circular polarization shift to the short wave region, and those with right hand circular polarization shift to the long wave region .

Conclusions

In conclusion, we investigated reflection spectra peculiarities of stack of right- and left-handed chiral photonic crystal layers providing important insights into self-assembled photonic crystal applications for adaptive micro-scale optical devices (consisting of a stack of right and left handed cholesteric liquid crystal layers). The system was shown to have multiple PBGs allowing for application particularly within the display industry. Conventional side-by-side red, green and blue color filters yield a loss of two-thirds of the incident light. The alternative of stacking cyan, magenta and yellow layers is also challenging—a 10% loss per layer compounds to nearly 50% overall. The subject system, however, can give three colors without any loss. Taking into account the possibility of tuning the width, number and frequency location of these regions by external (electric, magnetic, mechanical, thermal or light) fields, or by change of the internal structure of the system, such systems appear to have prospects.

The considered system can have also applications as tunable optical filters or mirrors. The subject system can be used for obtaining a 100% polarized radiation from a non-polarized system without any loss.

References

[1] Nader, E., & Richard, W. Z., (Eds.). (2006). *Metamaterials: Physics and Engineering Explorations*, Wiley-IEEE Press. p. 440.
[2] Ramakrishna, S. A., & Grzegorczyk, T. M. (2009). *Physics and Applications of Negative Refractive Index Materials*, Taylor & Francis Group.
[3] Cai, W., & Shalaev, V. (2010). *Optical Metamaterials*, Springer.
[4] Joannopoulos, J., Meade, R., & Winn, J. (1995). *Photonic Crystals*, Princeton Univ.: Princeton.
[5] Sakoda, K. (2001). *Optical Properties of Photonic Crystals*, Springer: Berlin.
[6] Johnson, S. G., & Joannopoulos, J. (2002). *Photonic Crystals: The Road from Theory to Practice*, Kluwer: Boston.

[7] Soukoulis, C. M. (Ed.). (2001). *Photonic Crystals and Light Localization in the 21st Century*, NATO Science Series C: Vol. 563, p. 616.
[8] Ha, N. Y., Takanishi, Y., Ishikawa, K., & Takezoe, H. (2007). *Opt. Express.*, *15*, 1024.
[9] Ha, N. Y., Ohtsuka, Y., Jeong, S. M., Nishimura, S., Suzaki, G., Takanishi, Y., Ishikawa, K., & Takezoe, H. (2008). *Nature Mat.*, *7*, 43.
[10] Nascimento, E. M., de Oliveira, I. N., & Lyra, M. L. (2008). *J. Appl. Phys.*, *104*, 103511.
[11] Nascimento, E. M., Zanetti, F. M., Lyra, M. L., & de Oliveira, I. N. (2010). *Phys. Rev. E.*, *81*, 031713.
[12] Ha, N. Y., Jeong, S. M., Nishimura, S., & Takezoe, H. (2010). *Adv. Matter.*, *22*, 1617.
[13] He, Z., Ye, Z., Cui, Q., Zhu, J., Gao, H., Ling, Y., Cui, H., Lu, J., Gao, X., & Su, Y. (2011) *Opt. Commun.*, *284*, 4022.
[14] Gevorgyan, A. H. (2011). *Phys. Rev. E.*, *83*, 011702.
[15] Gevorgyan, A. A., Papoyan, K. V., & Pikichyan, O. V. (2000). *Opt. Spectrosc.*, *88*, 586.
[16] Mitov, M., & Dessaud, N. (2006). *Nature Mat.*, *5*, 361.
[17] Mitov, M., & Dessaud, N. (2007). *Liq. Cryst.*, *34*, 183.
[18] Takanishi, Y., Ohtsuka, Y., Suzaki, G., Nishimara, S., & Takazoe, H. (2010). *Opt. Express.*, *18*, 12909.
[19] Robbie, K., Brett, M. J., & Lakhtakia, A. (1996). *Nature*, *384*, 616.
[20] Hodgkinson, I. J., Wu, Q. H., Knight, B., Lakhtakia, A., & Robbie, K. (2000). *Appl. Opt.*, *39*, 642.
[21] Jeng, S.-C., Hwang, S.-J., Hung, Y.-H., & ??? S.-C. (2010). *Chen. Opt. Express*, *18*, 22572.
[22] Vardanyan, G. A., & Gevorgyan, A. A. (1997). *Crystallography Reports*, *42*, 663.
[23] Gevorgyan, A. A. (2000). *Optics and Spectroscopy*, *89*, 631.
[24] Azzam, R. M. A., & Bashara, N. M. (1977). *Ellipsometry and Polarized Light*, North-Holland, NY.